On wave families in a two-layer falling film

Çekiç, G.; Sisoev, Grigory

DOI:
10.1016/j.ijnonlinmec.2014.11.020

Document Version
Peer reviewed version

Citation for published version (Harvard):
Çekiç, G & Sisoev, G 2015, 'On wave families in a two-layer falling film', *International Journal of Non-Linear Mechanics*, vol. 69, pp. 45-54. https://doi.org/10.1016/j.ijnonlinmec.2014.11.020

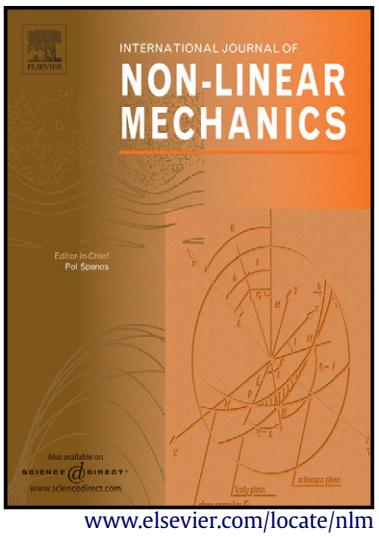

On wave families in a two-layer falling film

G. Çekiç, G.M. Sisoev

PII: S0020-7462(14)00236-4
DOI: http://dx.doi.org/10.1016/j.ijnonlinmec.2014.11.020
Reference: NLM2418

www.elsevier.com/locate/nlm

To appear in: *International Journal of Non-Linear Mechanics*

Received date: 21 August 2014
Accepted date: 9 November 2014

Cite this article as: G. Çekiç, G.M. Sisoev, On wave families in a two-layer falling film, *International Journal of Non-Linear Mechanics,* http://dx.doi.org/10.1016/j.ijnonlinmec.2014.11.020

On wave families in a two-layer falling film

G. Çekiç

School of Mathematics, University of Birmingham, Birmingham B15 2TT, United Kingdom

G. M. Sisoev

School of Mathematics, University of Birmingham, Birmingham B15 2TT, United Kingdom

Abstract

Using an approximate method, families of nonlinear steady-traveling periodic waves in a two-layer falling film have been found for the first time. Computed waves have qualitatively similar behavior as that of those found in homogeneous films but the quantitative characteristics of the waves strongly depend on additional similarity parameters in the two-layer films. In particular, the average location of the interface affects the bifurcation scheme of the waves.

Key words: thin fluid film, interface, nonlinear waves, bifurcations

1 Introduction

Interest in two-layer (and multilayer) films is stimulated by applications, in particular, in technologies providing mass transfer between two liquids. Due to difficulty of the problem, most attention has been paid to linear models and weakly nonlinear models.

Long wave instability of the two-layer flow was studied in [1] in the case of equal dynamic viscosities and different densities of the liquids. The asymptotic method developed in [2] was used to analyze the dependence of the neutral curves for the surface mode on the density ratio and the depth ratio. The interface mode was analyzed in [3], and the general case of both modes in flow with viscous stratification was considered in [4] using the same method.

Email address: g.sisoev@bham.ac.uk (G. M. Sisoev).

The linear stability at arbitrary values of the similarity parameters was investigated for the first time in [5] where the generalized Orr-Sommerfeld problem was solved numerically. Two unstable modes associated with the free surface and the interface were computed at moderate values of the Reynolds number. It has been shown that the interface mode corresponds to the Rayleigh-Taylor instability depending on the ratio of the liquids' densities in the case of small wall inclination. It was also found that the interface mode is unstable if the less viscous liquid is in the layer adjacent to the free surface, and this mode is stable if this liquid is adjacent to the solid substrate.

Later the Orr-Sommerfeld problem was used in [6] to investigate the interface and surface modes without taking into account both interface and surface tensions, or the surface tension only. In [7,8] the temporal and spatial growth rates were also calculated without considering the interface and surface tensions. In particular, the result of [5] about the absolute instability in the two-layer flow as the Rayleigh-Taylor instability was confirmed.

The limit case of zero value of the Reynolds number and absence of the surface and interface tension was analyzed in [9] using an asymptotic method. Mechanism of the surface and long interfacial waves was discussed in [10,11] at zero and very low values of the Reynolds number.

In parallel with the papers directly dealing with the gravity-driven two-layer film flow, there are many works dealing with two types of flows, falling films and interface waves, which are relevant to the considered problem.

Film flow down a vertical plane at moderate flow rates, or a falling film, has been considered in numerous experimental and theoretical investigations. Falling films demonstrate a wide variety of flow regimes, which are very sensitive to flow conditions. The first systematic experimental investigations [12] demonstrated the existence of two principal wave types: periodic sinusoidal waves and solitary waves, traveling with constant velocity. These so-called regular waves can take on different shapes, amplitudes and velocities depending on flow conditions.

The principal method of theoretical investigation based on use of a thin layer approximation was suggested in [13]. The majority of theoretical results used to describe experimental data were reached in the framework of the Kapitza-Shkadov evolution equations derived in [14] by the integral method. In particular, numerous types of steady-traveling waves in the framework of this approximation, see [15–23] and references in these publications, have been computed. Detailed description of the film theory can be found in monographs [24,25].

Another relevant area of research is the interface instability between two viscous flows. This type of instability was first studied in [26] by the asymptotic method [2] in the case of the plane Couette-Poiseulle flow. In a specific case

of liquids with equal densities, it was shown that the flow is unstable for any small value of the Reynolds number, and the instability is supplied by either the moving boundary or the pressure gradient. In [27], a parallel flow of two viscous liquids of equal density in infinite domains divided by a flat interface was studied, and it was shown that there exists a short wave instability in the absence of the surface tension. This mechanism of instability is comparatively small, and it can be stabilized by the surface tension. As illustrated in [28], the interface tension should be unrealistically small to observe the interface instability in the unbounded stratified Couette flow. In the case when one of liquids is bounded by a wall, and another liquid is unbounded, there were found a long wave interface instability in [29]. In [30], a weakly nonlinear equation modeling the plane Couette-Poiseulle flow of two liquids was derived, and some examples of wave evolution were computed. A special case of the two-layer Couette flow with high dynamic viscosities ratios was modeled in [31] using an evolution equation derived by the integral method. The integral method was also used to model non-linear solitary waves in two-layer plane flows driven by the gravity [32] and the pressure [33]. Some attention was also paid to stability of interface waves in [34] where a gas-liquid waves were studied. Solitary and periodic waves in an interface between two-liquids were observed in a cylindrical Couette flow at high ratio of the dynamic viscosities [35] and a microchannel [36].

In this paper, we use the integral method to find steady-traveling periodic waves in the two-layer film flow.

This paper is organized as follows: In Section 2, the evolution equations are derived to model flows at real-life values of the similarity parameters. In Section 3, the method used to compute steady-traveling waves is given, and examples of the waves are shown. Finally, conclusions are provided in Section 4.

2 Evolution equations

2.1 Equations and boundary conditions

To model two-layer film flowing down on a vertical wall, the Cartesian coordinate system (x, y) is introduced with the x-axis pointed down and y-axis pointed into the film bulk. We assume that both liquids are immiscible, incompressible and viscous, and we will refer the liquid attached to the wall as '1' and the liquid having the free surface as '2'.

The flow is described by the full Navier-Stokes equations and relevant boundary conditions for the velocity components u and v corresponding to the axis

x and y, respectively, the pressure p , the first layer thickness $h^{(1)}$ and the film thickness $h^{(2)}$. To formulate the equations and boundary conditions in the dimensionless form, we take film thickness H_c of the waveless flow as the length scale, and the average film velocity $U_c = Q_c/H_c$, where Q_c is the total flow rate of the film, as the velocity scale. Then dimensional variables are converted into dimensionless form as,

$$t \to \frac{H_c}{\kappa U_c} t, \quad \left(x, y, h^{(1)}, h^{(2)}\right) \to H_c \left(\frac{x_\kappa}{\kappa}, y, h^{(1)}, h^{(2)}\right),$$
$$(u, v) \to U_c \left(u, \kappa v_\kappa\right), \quad p \to \rho^{(2)} U_c^2 p,$$

where κ is the stretching parameter defined below.

The dimensionless Navier-Stokes equations and the problem boundary conditions are written in the form

$$\frac{\partial u}{\partial x_\kappa} + \frac{\partial v_\kappa}{\partial y} = 0, \tag{1}$$
$$\frac{\partial u}{\partial t_\kappa} + u\frac{\partial u}{\partial x_\kappa} + v_\kappa \frac{\partial u}{\partial y} = -\frac{1}{\rho_0^{(j)}}\frac{\partial p}{\partial x_\kappa} + \frac{\nu_0^{(j)}}{\kappa \mathrm{Re}}\left(\kappa^2 \frac{\partial^2 u}{\partial x_\kappa^2} + \frac{\partial^2 u}{\partial y^2}\right) + \frac{1}{\kappa \mathrm{Fr}^2},$$
$$\kappa^2\left(\frac{\partial v_\kappa}{\partial t_\kappa} + u\frac{\partial v_\kappa}{\partial x_\kappa} + v_\kappa \frac{\partial v_\kappa}{\partial y}\right) = -\frac{1}{\rho_0^{(j)}}\frac{\partial p}{\partial y} + \frac{\kappa^2 \nu_0^{(j)}}{\kappa \mathrm{Re}}\left(\kappa^2 \frac{\partial^2 v_\kappa}{\partial x_\kappa^2} + \frac{\partial^2 v_\kappa}{\partial y^2}\right),$$
$$y = 0: \quad u = 0, \quad v_\kappa = 0,$$
$$y = h^{(1)}(x_\kappa, t_\kappa): \quad \frac{\partial h^{(1)}}{\partial t_\kappa} + u\frac{\partial h^{(1)}}{\partial x_\kappa} = v_\kappa, \quad [p_{nn}]_1^2 + \frac{\kappa^2 \sigma_0 \varsigma_\kappa^{(1)}}{\mathrm{We}} = 0,$$
$$[p_{n\tau}]_1^2 = 0, \quad [u]_1^2 = 0, \quad [v_\kappa]_1^2 = 0,$$
$$y = h^{(2)}(x_\kappa, t_\kappa): \quad \frac{\partial h^{(2)}}{\partial t_\kappa} + u\frac{\partial h^{(2)}}{\partial x_\kappa} = v_\kappa, \quad p_{nn} - \frac{\kappa^2 \varsigma_\kappa^{(2)}}{\mathrm{We}} = 0, \quad p_{n\tau} = 0,$$

where the notation $[f]_1^2 \equiv f_2 - f_1$ denotes the jump in quantity f from the value in the first liquid, $f^{(1)}$, to the value in the second, $f^{(2)}$. The boundary conditions in (1) include the normal, p_{nn}, and tangential, $p_{n\tau}$, stresses and the curvatures ς_κ which are calculated as follows

$$p_{nn} = -p + \frac{2\kappa^2 \rho_0^{(j)} \nu_0^{(j)}}{\kappa \mathrm{Re}}\left[1 + \kappa^2\left(\frac{\partial h}{\partial x_\kappa}\right)^2\right]^{-1} \times$$
$$\left[\left(1 - \kappa^2\left(\frac{\partial h}{\partial x_\kappa}\right)^2\right)\frac{\partial v_\kappa}{\partial y} - \frac{\partial h}{\partial x_\kappa}\left(\frac{\partial u}{\partial y} + \kappa^2 \frac{\partial v_\kappa}{\partial x_\kappa}\right)\right], \tag{2}$$
$$p_{n\tau} = \frac{\rho_0^{(j)} \nu_0^{(j)}}{\mathrm{Re}}\left[1 + \kappa^2\left(\frac{\partial h}{\partial x_\kappa}\right)^2\right]^{-1} \times$$

$$\left[\left(1-\kappa^2\left(\frac{\partial h}{\partial x_\kappa}\right)^2\right)\left(\frac{\partial u}{\partial y}+\kappa^2\frac{\partial v_\kappa}{\partial x_\kappa}\right)+4\kappa^2\frac{\partial h}{\partial x_\kappa}\frac{\partial v_\kappa}{\partial y}\right],$$

$$\varsigma_\kappa=\left[1+\kappa^2\left(\frac{\partial h}{\partial x_\kappa}\right)^2\right]^{-\frac{3}{2}}\frac{\partial^2 h}{\partial x_\kappa^2}.$$

The system (1) and (2) contains the following dimensionless parameters:

$$\mathrm{Re}=\frac{U_c H_c}{\nu^{(2)}},\quad \mathrm{We}=\frac{\rho^{(2)}U_c^2 H_c}{\sigma^{(2)}},\quad \mathrm{Fr}^2=\frac{U_c^2}{gH_c},$$
$$\rho_0=\frac{\rho^{(1)}}{\rho^{(2)}},\quad \nu_0=\frac{\nu^{(1)}}{\nu^{(2)}},\quad \sigma_0=\frac{\sigma^{(1)}}{\sigma^{(2)}},$$

with $\rho_0^{(2)}=1$, $\rho_0^{(1)}=\rho_0$, $\nu_0^{(2)}=1$ and $\nu_0^{(1)}=\nu_0$, where $\rho^{(j)}$ and $\nu^{(j)}$, $j=1,2$ are the densities and viscosities of the liquids, respectively, $\sigma^{(1)}$ and $\sigma^{(2)}$ are the interface and surface tensions, and g is gravity.

The system (1) and (2) has a solution, denoted by capital letters below, describing the steady waveless flow:

$$y\in[0,H]:\ U^{(1)}=\frac{\mathrm{Re}}{\nu_0\mathrm{Fr}^2}\left(a^{(1)}y-\frac{y^2}{2}\right),\ V^{(1)}=0,\ P^{(1)}=0,$$
$$y\in[H,1]:\ U^{(2)}=\frac{\mathrm{Re}}{\mathrm{Fr}^2}\left(a^{(2)}+y-\frac{y^2}{2}\right),\ V^{(2)}=0,\ P^{(2)}(y)=0,$$

where the coefficients

$$a^{(1)}=\frac{1}{\rho_0}+\left(1-\frac{1}{\rho_0}\right)H,\ a^{(2)}=\left(\frac{1+\nu_0}{2\nu_0}-\frac{1}{\rho_0\nu_0}\right)H^2+\left(\frac{1}{\rho_0\nu_0}-1\right)H$$

have been used. Then the flow rates in the first layer, $Q^{(1)}$, and the second layer, Q, are calculated

$$Q^{(1)}=\int_0^H U^{(1)}dy=\frac{\mathrm{Re}\ H^2}{2\nu_0\mathrm{Fr}^2}\left[\frac{1}{\rho_0}+\left(\frac{2}{3}-\frac{1}{\rho_0}\right)H\right],\tag{3}$$
$$Q=\int_H^1 U^{(2)}dy$$
$$=\frac{\mathrm{Re}\ (1-H)}{\mathrm{Fr}^2}\left[\frac{1}{3}+\left(\frac{1}{\rho_0\nu_0}-\frac{2}{3}\right)H+\left(\frac{1}{3}+\frac{1}{2\nu_0}-\frac{1}{\rho_0\nu_0}\right)H^2\right].$$

Finally, we find the total flow rate in the two-layer film

$$
\begin{aligned}
&Q^{(2)} = Q^{(1)} + Q = \frac{\varphi \mathrm{Re}}{\mathrm{Fr}^2}, \\
&\varphi = \frac{H^2}{2\nu_0}\left[\frac{1}{\rho_0} + \left(\frac{2}{3} - \frac{1}{\rho_0}\right) H\right] \\
&\quad + (1-H)\left[\frac{1}{3} + \left(\frac{1}{\rho_0\nu_0} - \frac{2}{3}\right) H + \left(\frac{1}{3} + \frac{1}{2\nu_0} - \frac{1}{\rho_0\nu_0}\right) H^2\right].
\end{aligned}
$$

Since we have taken the average velocity of the waveless flow as the velocity scale, the dimensionless total flow rate is $Q^{(2)} = 1$ and thus $\mathrm{Fr}^2 = \varphi \mathrm{Re}$. This relation allows us to eliminate the Froude number, and calculate the scale velocity $U_c = \varphi g H_c^2 / \nu^{(2)}$.

In the theory of thin films, the Reynolds number and the Weber number are replaced with the Kapitza number, Ka, and the film parameter, δ, which can be defined for the two-layer film as

$$
\mathrm{Ka} \equiv \frac{\sigma^{(2)}}{\rho^{(2)}\left(g\left(\nu^{(2)}\right)^4\right)^{\frac{1}{3}}}, \quad \delta \equiv \frac{1}{45\left(\nu^{(2)}\right)^2}\left(\frac{\rho^{(2)} g^4 H_c^{11}}{\sigma^{(2)}}\right)^{\frac{1}{3}}.
$$

Then the original parameters are re-calculated:

$$
\mathrm{Re} = \varphi\,(45\delta)^{\frac{9}{11}}\,\mathrm{Ka}^{\frac{3}{11}}, \quad \mathrm{We} = \frac{\varphi^2\,(45\delta)^{\frac{15}{11}}}{\mathrm{Ka}^{\frac{6}{11}}}.
$$

2.2 Approximate system

Wave regimes in film flows are observed under conditions when there is a balance of the gravity, viscosity and capillarity. Acting in opposite directions, the gravity and viscosity form a flow with some average parameters. As known from experiments and observations, this flow is unstable and it leads to the development of wave regimes whose parameters depend on the capillarity competing with the gravity and the viscosity. It can be formulated as a balance of the following terms in the equations (1):

$$
\frac{1}{\kappa\varphi\mathrm{Re}} = \frac{\kappa^2}{\mathrm{We}}, \tag{4}
$$

Liquid	Density, g/cm^3	Kinematic viscosity, cm^2/s	Surface tension with air, g/s^2
Water	0.998	0.0101	72
Benzene	0.879	0.0074	29

Table 1
Physical properties of water and benzene. The interface tension between water and benzene is 33.6 g/s^2.

where, taking into account the formula derived above for the Froude number, the left-hand side is the gravity term in the x-momentum equation in (1), and the right-hand side characterizes the pressure gradient induced by the surface tension on the free surface. Equation (4) allows us to find the stretching parameter κ:

$$\kappa = \left(\frac{\rho^{(2)} g H_c^2}{\sigma^{(2)}}\right)^{\frac{1}{3}} = \left(\frac{(45\delta)^2}{\mathrm{Ka}^3}\right)^{\frac{1}{11}}.$$

The method of using the longitudinal wave scale to derive an approximate equations to model thin film flows was successfully applied in [14] and numerous succeeding works for one-layer films [24,25], and we can expect that it should also give a good approximation in two-layer film flows if the properties of the liquids are close each other. On the other hand, the surface instability and the interface instabilities have different length scales, and the accuracy of the approximation can be relatively worse in comparison with the homogeneous film.

It is worth to note that the parameter κ can also be written in the form $\kappa = (\mathrm{Ca}/\varphi)^{1/3}$ where the capillary number $\mathrm{Ca} \equiv \rho^{(2)}\nu^{(2)}U_c/\sigma^{(2)} = \mathrm{We}/\mathrm{Re}$ has been used.

For many liquids, including water, the Kapitza number is sufficiently large, and it leads to small values of the stretching parameter $\kappa^2 \ll 1$ in homogeneous films at moderate values of the Reynolds number [22]. As an example of two-layer film, in this paper we consider the case of water (liquid 1) and benzene (liquid 2) whose physical properties are summarized in Table 1.

Fig. 1 demonstrates an example of values κ^2 and Re. It is seen that $\kappa^2 \leq 0.05$ if $\delta \leq 0.4$ at $H = 0.3$. For the same interval of δ, the Reynolds number $\mathrm{Re} \leq 25$ which is typical for observed regular waves in film flows.

Due to the small values of κ^2, we can neglect terms of order $O(\kappa^2)$ in (1) and (2), and then the system is re-written as follows:

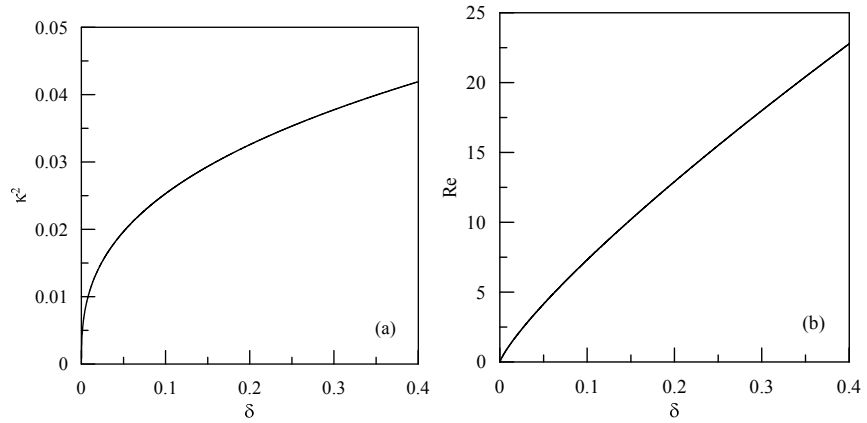

Fig. 1. Dependencies of the stretching parameter κ^2 (a) and the Reynolds number Re (b) on the film parameter δ in the case water-benzene system at $H = 0.3$.

$$
\begin{aligned}
&\frac{\partial u}{\partial x_\kappa} + \frac{\partial v_\kappa}{\partial y} = 0, \qquad (5)\\
&\frac{\partial u}{\partial t_\kappa} + u\frac{\partial u}{\partial x_\kappa} + v_\kappa\frac{\partial u}{\partial y} = -\frac{1}{\rho_0^{(j)}}\frac{\partial p}{\partial x_\kappa} + \frac{\varphi\nu_0^{(j)}}{5\delta}\frac{\partial^2 u}{\partial y^2} + \frac{1}{5\delta},\\
&\frac{\partial p}{\partial y} = 0,\\
&y = 0: \quad u = 0, \quad v_\kappa = 0,\\
&y = h^{(1)}(x_\kappa, t_\kappa): \quad \frac{\partial h^{(1)}}{\partial t_\kappa} + u\frac{\partial h^{(1)}}{\partial x_\kappa} = v_\kappa, \quad [u]_1^2 = 0, \quad [v_\kappa]_1^2 = 0,\\
&\qquad\qquad \left[\rho_0^{(j)}\nu_0^{(j)}\frac{\partial u}{\partial y}\right]_1^2 = 0, \quad [-p]_1^2 + \frac{\sigma_0}{5\delta}\frac{\partial^2 h^{(1)}}{\partial x_\kappa^2} = 0,\\
&y = h^{(2)}(x_\kappa, t_\kappa): \quad \frac{\partial h^{(2)}}{\partial t_\kappa} + u\frac{\partial h^{(2)}}{\partial x_\kappa} = v_\kappa, \quad \frac{\partial u}{\partial y} = 0, \quad p + \frac{1}{5\delta}\frac{\partial^2 h^{(2)}}{\partial x_\kappa^2} = 0
\end{aligned}
$$

where we have used that $\delta = \kappa\varphi\mathrm{Re}/5$.

The y-momentum equations in the layers and the boundary conditions for the normal stresses allow us to eliminate the pressures from the system:

$$
p^{(1)} = -\frac{1}{5\delta}\left(\sigma_0\frac{\partial^2 h^{(1)}}{\partial x_\kappa^2} + \frac{\partial^2 h^{(2)}}{\partial x_\kappa^2}\right), \quad p^{(2)} = -\frac{1}{5\delta}\frac{\partial^2 h^{(2)}}{\partial x_\kappa^2}.
$$

Having substituted these formulas into the x-momentum equations and then integrating them as well as the continuity equations across each layer, we arrive at the following evolution system

$$\frac{\partial h^{(1)}}{\partial t_\kappa}+\frac{\partial q^{(1)}}{\partial x_\kappa}=0,\quad q^{(1)}\equiv\int\limits_0^{h^{(1)}}u\;dy,$$

$$\frac{\partial q^{(1)}}{\partial t_\kappa}+\frac{\partial}{\partial x_\kappa}\int\limits_0^{h^{(1)}}u^2\;dy$$
$$=\frac{1}{5\delta}\left[\frac{\sigma_0 h^{(1)}}{\rho_0}\frac{\partial^3 h^{(1)}}{\partial x_\kappa^3}+\frac{h^{(1)}}{\rho_0}\frac{\partial^3 h^{(2)}}{\partial x_\kappa^3}+\varphi\nu_0\left(\left.\frac{\partial u}{\partial y}\right|_{h^{(1)}}-\left.\frac{\partial u}{\partial y}\right|_0\right)+h^{(1)}\right],$$

$$\frac{\partial\left(h^{(2)}-h^{(1)}\right)}{\partial t_\kappa}+\frac{\partial q}{\partial x_\kappa}=0,\quad q\equiv\int\limits_{h^{(1)}}^{h^{(2)}}u\;dy,$$

$$\frac{\partial q}{\partial t_\kappa}+\frac{\partial}{\partial x_\kappa}\int\limits_{h^{(1)}}^{h^{(2)}}u^2\;dy$$
$$=\frac{1}{5\delta}\left[\left(h^{(2)}-h^{(1)}\right)\frac{\partial^3 h^{(2)}}{\partial x_\kappa^3}+\varphi\left(\left.\frac{\partial u}{\partial y}\right|_{h^{(2)}}-\left.\frac{\partial u}{\partial y}\right|_{h^{(1)}}\right)+h^{(2)}-h^{(1)}\right],$$

where $q^{(1)}(x_\kappa,t_\kappa)$ and $q(x_\kappa,t_\kappa)$ are local flow rates in the layers. To calculate the integrals in the left-hand sides and viscous terms in the right-hand sides of the momentum equations, we approximate the velocity profiles by the following parabolic functions:

$$y\in\left[0,h^{(1)}\right]:\quad u=U_{11}y+U_{12}y^2,\tag{6}$$
$$U_{12}=\frac{3}{h^{(1)}\left[\left(3-4\rho_0\nu_0\right)h^{(1)}+4\rho_0\nu_0h^{(2)}\right]}$$
$$\times\left\{\frac{3q^{(2)}}{h^{(2)}-h^{(1)}}-\left[\frac{3}{h^{(2)}-h^{(1)}}+\frac{2}{\left(h^{(1)}\right)^2}\left[\left(3-\rho_0\nu_0\right)h^{(1)}+\rho_0\nu_0h^{(2)}\right]\right]q^{(1)}\right\},$$
$$U_{11}=\frac{2q^{(1)}}{\left(h^{(1)}\right)^2}-\frac{2h^{(1)}U_{12}}{3},$$
$$y\in\left[h^{(1)},h^{(2)}\right]:\quad u=U_{20}+U_{22}\left(y^2-2h^{(2)}y\right),$$
$$U_{22}=-\frac{\rho_0\nu_0}{2}\frac{U_{11}+2U_{12}h^{(1)}}{h^{(2)}-h^{(1)}},$$
$$U_{20}=\frac{q^{(2)}-q^{(1)}}{h^{(2)}-h^{(1)}}+\frac{1}{3}\left[2\left(h^{(2)}\right)^2+2h^{(1)}h^{(2)}-\left(h^{(1)}\right)^2\right]U_{22}.$$

The approximating solution (6) satisfies the boundary conditions in (5), and provides the flow rates $q^{(1)}$ and $q^{(2)}\equiv q^{(1)}+q$ in the first layer and the whole film, respectively. Finally, we derive the evolution equations for $h^{(1)}$, $q^{(1)}$, $h^{(2)}$ and $q^{(2)}$:

$$
\begin{aligned}
&\frac{\partial h^{(1)}}{\partial t_\kappa}+\frac{\partial q^{(1)}}{\partial x_\kappa}=0, \\
&\frac{\partial q^{(1)}}{\partial t_\kappa}+\frac{\partial J^{(1)}}{\partial x_\kappa}=\frac{h^{(1)}}{5\delta}\left(\frac{\sigma_0}{\rho_0}\frac{\partial^3 h^{(1)}}{\partial x_\kappa^3}+\frac{1}{\rho_0}\frac{\partial^3 h^{(2)}}{\partial x_\kappa^3}+2\varphi\nu_0 U_{12}+1\right), \\
&\frac{\partial h^{(2)}}{\partial t_\kappa}+\frac{\partial q^{(2)}}{\partial x_\kappa}=0, \\
&\frac{\partial q^{(2)}}{\partial t_\kappa}+\frac{\partial J^{(2)}}{\partial x_\kappa}=\frac{1}{5\delta}\left[\frac{\sigma_0 h^{(1)}}{\rho_0}\frac{\partial^3 h^{(1)}}{\partial x_\kappa^3}+\left(h^{(2)}+\left(\frac{1}{\rho_0}-1\right)h^{(1)}\right)\frac{\partial^3 h^{(2)}}{\partial x_\kappa^3}\right] \\
&\quad+\frac{\varphi}{5\delta}\left[2\nu_0 U_{12}h^{(1)}\left(1-\rho_0\right)-\rho_0\nu_0 U_{11}\right]+\frac{h^{(2)}}{5\delta},
\end{aligned}
\tag{7}
$$

where

$$
\begin{aligned}
J^{(1)} &= \left(h^{(1)}\right)^3\left[\frac{U_{11}^2}{3}+\frac{U_{11}U_{12}}{2}h^{(1)}+\frac{U_{12}^2}{5}\left(h^{(1)}\right)^2\right], \\
J^{(2)} &= J^{(1)}+U_{20}^2\left(h^{(2)}-h^{(1)}\right)-2U_{20}U_{22}h^{(2)}\left[\left(h^{(2)}\right)^2-\left(h^{(1)}\right)^2\right]+ \\
&\quad\frac{2}{3}\left[2U_{22}^2\left(h^{(2)}\right)^2+U_{20}U_{22}\right]\left[\left(h^{(2)}\right)^3-\left(h^{(1)}\right)^3\right]- \\
&\quad U_{22}^2h^{(2)}\left[\left(h^{(2)}\right)^4-\left(h^{(1)}\right)^4\right]+\frac{U_{22}^2}{5}\left[\left(h^{(2)}\right)^5-\left(h^{(1)}\right)^5\right].
\end{aligned}
\tag{8}
$$

The system contains the film parameter δ, the parameters σ_0, ρ_0 and ν_0 characterizing physical properties of the liquids, and the parameter H depending on the waveless interface location for given flow rates in the layers.

2.3 Linear stability analysis

We start from the linear stability analysis of the steady waveless flow to find the domain of instability in the space of the similarity parameters. The results can be compared with the linear spectrum of the Orr-Sommerfeld problem for the Navier-Stokes system, (1) and (2).

The system (7) possesses a steady flow solution $h^{(1)}=H$ and $h^{(2)}=1$ satisfying the following equations:

$$
2\varphi\nu_0 U_{12}+1=0, \quad \varphi\left[2\nu_0 U_{12}h^{(1)}\left(1-\rho_0\right)-\rho_0\nu_0 U_{11}\right]+h^{(2)}=0. \tag{9}
$$

The flow rates $Q^{(1)}$ and Q in the layers are given by (3).

To analyze the linear stability of the steady flow, we look for a solution of (7) in the form of normal modes

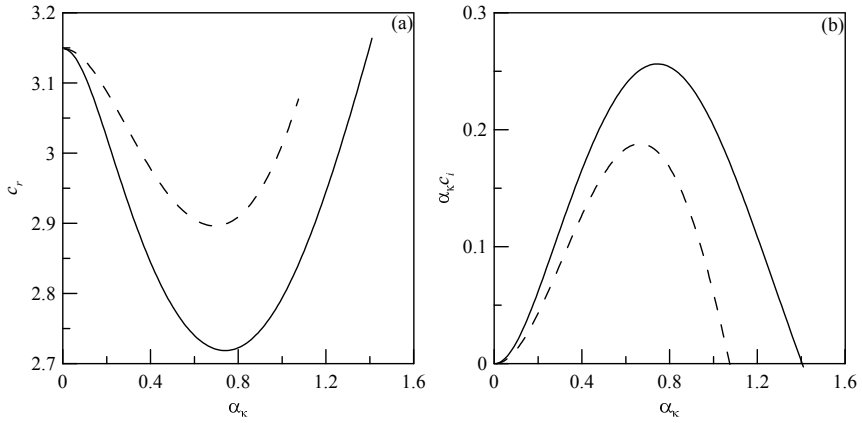

Fig. 2. Wave velocities (a) and amplification factors (b) for the surface mode in the water-benzene system at $\delta = 0.1$ and $H = 0.3$. Solid curves and dashed curves denote solutions of the approximate model (7) and the Orr-Sommerfeld problem for (1) and (2), respectively.

$$h^{(1)} = H + \breve{h}^{(1)} e^{i\alpha_\kappa (x_\kappa - c t_\kappa)}, \quad h^{(2)} = 1 + \breve{h}^{(2)} e^{i\alpha_\kappa (x_\kappa - c t_\kappa)},$$
$$q^{(1)} = Q^{(1)} + \breve{q}^{(1)} e^{i\alpha_\kappa (x_\kappa - c t_\kappa)}, \quad q^{(2)} = Q^{(2)} + \breve{q}^{(2)} e^{i\alpha_\kappa (x_\kappa - c t_\kappa)},$$

where variables with breves denote small amplitudes, α_κ is the wavenumber, and $c = c_r + ic_i$ is the complex velocity to be computed. Substituting this solution into (7) and linearizing lead to the characteristic equation for the eigenvalue c

$$b_4 c^4 + b_3 c^3 + b_2 c^2 + b_1 c + b_0 = 0, \tag{10}$$

where formulas for the coefficients $b_0, \ldots, b_4$ have been omitted for the sake of brevity.

As noted in Section 1, the two-layer film flow has two unstable modes at moderate flow rates. Figs. 2 and 3 show the wave velocity c_r and amplification factor $\alpha_\kappa c_i$ in the case of water-benzene system at $H = 0.3$ and $\delta = 0.1$ (Re $= 7.3$). In dimensional terms, this example corresponds to the film of the thickness $H_c = 0.116$ mm and the average velocity $U_c = 4.66$ cm/s. In parallel with the solutions of (10), Figs. 2 and 3 shows the results of the Orr-Sommerfeld problem [5].

It is seen that the model (7) provides a good approximation of the intervals of instability and wave velocities of both modes. This is a typical case for homogeneous film flows, and successful applications of the integral method are explained by the fact that real-life waves are usually observed for $\alpha_\kappa \le \alpha_{\kappa,n}/2$ where $\alpha_{\kappa,n}$ is the neutral wavenumber of the surface mode. In the considered case, eigenvalues of the surface mode computed in both models are also close but there is some discrepancy of the amplification factors of two models for the interface mode. However, we note that the scale of amplification factors of the

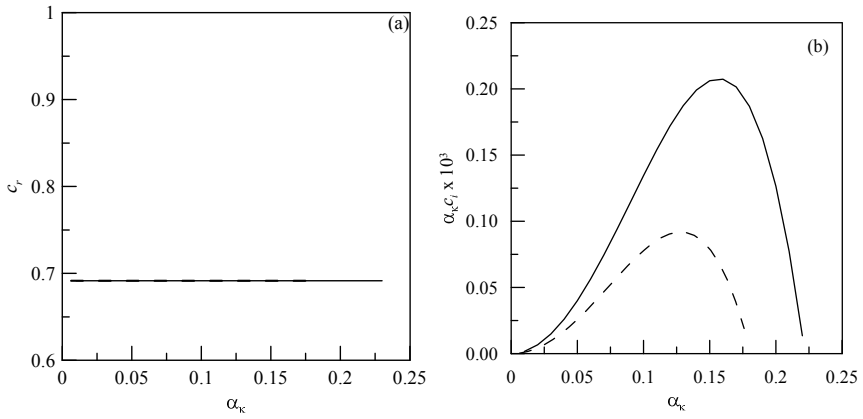

Fig. 3. Wave velocities (a) and amplification factors (b) for the interface mode waves in the water-benzene system at $\delta = 0.1$ and $H = 0.3$. Solid curves and dashed curves denote solutions of the approximate model (7) and the Orr-Sommerfeld problem for (1) and (2), respectively.

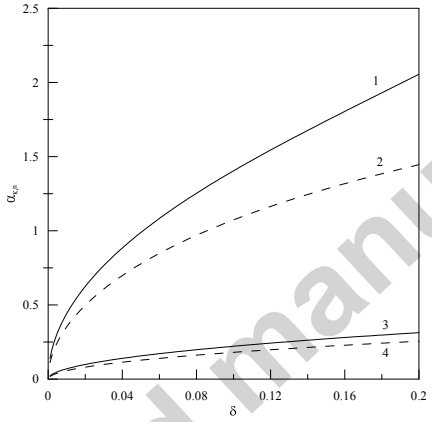

Fig. 4. Neutral curves of the surface mode (curves 1 and 2) and the interface mode (3 and 4) in the case of water-benzene system at $H = 0.3$. Curves 1 and 3 correspond to solutions of the approximate model (7), and curves 2 and 4 denote solutions of the Orr-Sommerfeld problem (1) and (2).

interface mode is about one thousand times smaller than ones of the surface mode. Even for such small values lying on the border of the method accuracy, the approximate model gives sufficiently good results, in particular as $\alpha_\kappa \to 0$. It is worthy to note that amplification factors of the interface mode can be comparable with that of the surface mode in films flowing down an incline whose inclination is relatively small [5] but we do not study non-vertical flows in this work.

Neutral curves of both modes are shown in Fig. 4. It is seen that the interface mode is unstable at relatively small values of the wavenumber. It indicates that the unstable interface modes can affect only very long waves.

3 Steady-traveling waves

3.1 Nonlinear eigenvalue problem

To find steady-traveling waves, we look for a solution of (7) in the form $h^{(1)}(\eta)$, $h^{(2)}(\eta)$, $q^{(1)}(\eta)$, $q^{(2)}(\eta)$ where $\eta = \alpha_\kappa (x_\kappa - ct_\kappa)$. Having substituted this solution and integrated the continuity equation to find the flow rates

$$q^{(1)} = ch^{(1)} + A^{(1)}, \quad q^{(2)} = ch^{(2)} + A^{(2)}, \tag{11}$$

where $A^{(1)}$ and $A^{(2)}$ are constants, we arrive at the following equations for the interface $h^{(1)}$ and the surface $h^{(2)}$:

$$\begin{aligned}
&-c^2\frac{dh^{(1)}}{d\eta} + \frac{dJ^{(1)}}{d\eta} \\
&\quad = h^{(1)}\left[\frac{1}{5\delta\alpha_\kappa}\left(\frac{\alpha_\kappa^3\sigma_0}{\rho_0}\frac{\partial^3 h^{(1)}}{d\eta^3} + \frac{\alpha_\kappa^3}{\rho_0}\frac{\partial^3 h^{(2)}}{d\eta^3} + 2\varphi\nu_0 U_{12} + 1\right)\right] \\
&-c^2\frac{dh^{(2)}}{d\eta} + \frac{dJ^{(2)}}{d\eta} = \frac{\alpha_\kappa^2}{5\delta}\left[\frac{\sigma_0 h^{(1)}}{\rho_0}\frac{\partial^3 h^{(1)}}{d\eta^3} + \left(h^{(2)} + \left(\frac{1}{\rho_0} - 1\right)h^{(1)}\right)\frac{\partial^3 h^{(2)}}{d\eta^3}\right] \\
&\quad + \frac{\varphi}{5\delta\alpha_\kappa}\left[2\nu_0 U_{12}h^{(1)}(1-\rho_0) - \rho_0\nu_0 U_{11}\right] + \frac{h^{(2)}}{5\delta\alpha_\kappa}
\end{aligned} \tag{12}$$

where the coefficients are given by (6) and (8).

Integrating both equations (11) over the period 2π allows us to find the constants $A^{(1)}$ and $A^{(2)}$:

$$A^{(1)} = q_0^{(1)} - ch_0^{(1)}, \quad A^{(2)} = q_0^{(2)} - ch_0^{(2)},$$

where

$$\begin{aligned}
h_0^{(1)} &= \frac{1}{2\pi}\int_0^{2\pi} h^{(1)}d\eta, \quad q_0^{(1)} = \frac{1}{2\pi}\int_0^{2\pi} q^{(1)}d\eta, \\
h_0^{(2)} &= \frac{1}{2\pi}\int_0^{2\pi} h^{(2)}d\eta, \quad q_0^{(2)} = \frac{1}{2\pi}\int_0^{2\pi} q^{(2)}d\eta.
\end{aligned}$$

Thus, the flow rates are

$$q^{(1)} = c\left(h^{(1)} - h_0^{(1)}\right) + q_0^{(1)}, \quad q^{(2)} = c\left(h^{(2)} - h_0^{(2)}\right) + q_0^{(2)}. \tag{13}$$

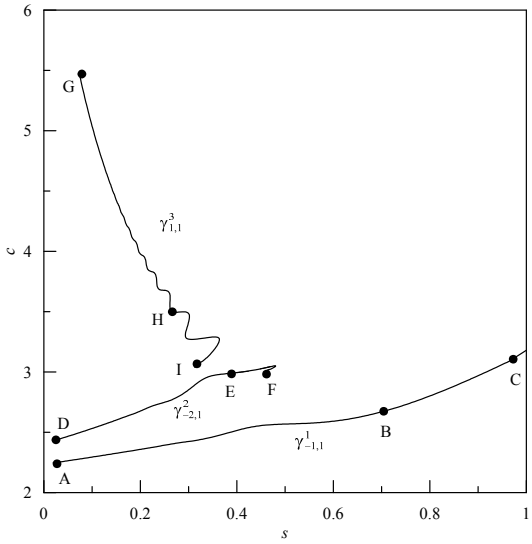

Fig. 5. Bifurcation scheme of the wave families at $\delta = 0.1$ and $H = 0.3$.

Equations (12) and (13) are accompanied by the periodic boundary conditions:

$$h^{(1)}\Big|_0 = h^{(1)}\Big|_{2\pi}, \quad \frac{dh^{(1)}}{d\eta}\Big|_0 = \frac{dh^{(1)}}{d\eta}\Big|_{2\pi}, \quad \frac{d^2h^{(1)}}{d\eta^2}\Big|_0 = \frac{d^2h^{(1)}}{d\eta^2}\Big|_{2\pi}, \qquad (14)$$
$$h^{(2)}\Big|_0 = h^{(2)}\Big|_{2\pi}, \quad \frac{dh^{(2)}}{d\eta}\Big|_0 = \frac{dh^{(2)}}{d\eta}\Big|_{2\pi}, \quad \frac{d^2h^{(2)}}{d\eta^2}\Big|_0 = \frac{d^2h^{(2)}}{d\eta^2}\Big|_{2\pi}.$$

Integrating (7) from 0 to 2π and using these periodic boundary conditions give us $h_0^{(1)} = H$ and $h_0^{(2)} = 1$.

Solutions of the eigenvalue problem (12), (13) and (14) for the first layer thicknesses $h^{(1)}$, the film thickness $h^{(2)}$, the wave velocity c and the flow rates $q^{(1)}$ and $q^{(2)}$ depend on the wavenumber α_κ, the similarity parameters δ, ρ_0, ν_0 and σ_0, and the relative thickness of the first layer H. It is convenient to use the normalized wavenumber $s \equiv \alpha_\kappa/\alpha_{\kappa,n}$ instead of the wavenumber α_κ itself.

3.2 Bifurcating wave families

In the theory of film flows, regular waves are sorted into families which are continuously parameterized by the normalized wavenumber s at given values of other similarity parameters, in this case δ, ρ_0, σ_0 and H. To identify the wave families we use the notation $\gamma^n_{\pm m,j}$, see [22,23].

Fig. 5 shows the bifurcation scheme of the families of nonlinear waves. Family $\gamma^1_{-1,1}$ bifurcates from the waveless flow at the neutral wavenumber as the first

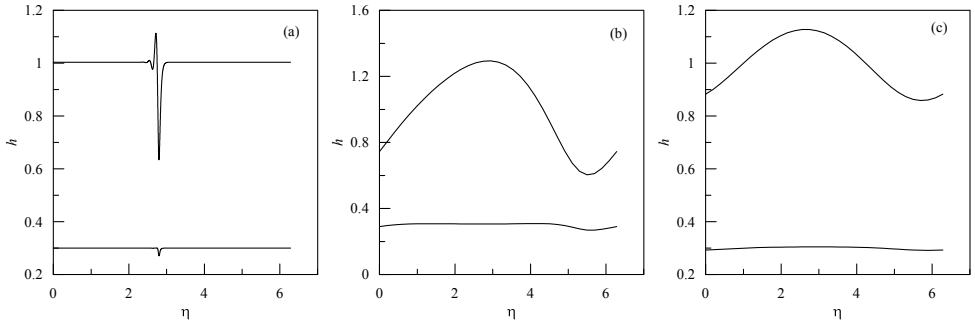

Fig. 6. Examples of waves belonging to the family $\gamma^1_{-1,1}$ at $s = 0.019$ (a), $s = 0.7$ (b) and $s = 0.9632$ (c). Panels (a), (b) and (c) correspond to the points A, B and C, respectively, in Fig. 5.

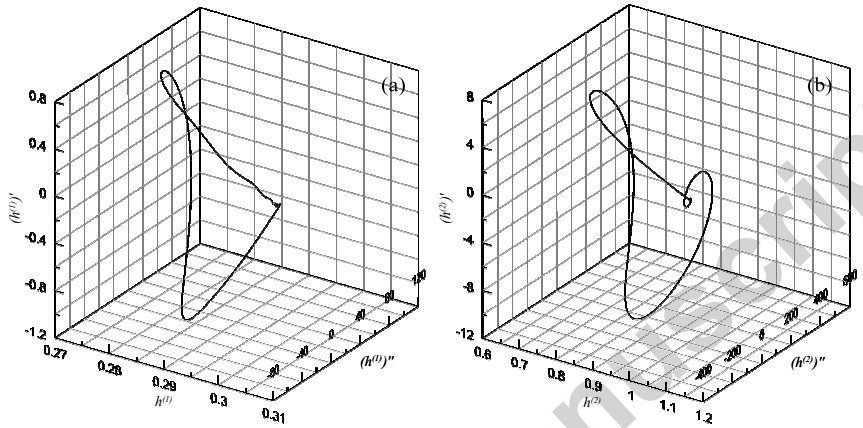

Fig. 7. Projections of 6-dimensional phase trajectory of the family $\gamma^1_{-1,1}$ in 3-dimensional subspace $\left(h^{(1)}, \left(h^{(1)}\right)', \left(h^{(1)}\right)''\right)$ (a) and $\left(h^{(2)}, \left(h^{(2)}\right)', \left(h^{(2)}\right)''\right)$ (b) , at $s = 0.019$, correspond to Fig. 6a.

harmonic, see Fig. 6c. As the wavenumber decreases, the surface wave amplitude grows, see Fig. 6b, and then the wave takes on a solitary-like shape with a long interval of constant thickness of the first layer and the film, see Fig. 6a. The surface shape shown in Fig. 6a is typical for long waves of the so-called first family [14] in a homogeneous film. We also note that the amplitude of the interfacial wave is small in comparison with the surface wave amplitude.

In Fig. 7, projections in 3-dimensional subspaces $\left(h^{(1)}, \left(h^{(1)}\right)', \left(h^{(1)}\right)''\right)$ and $\left(h^{(2)}, \left(h^{(2)}\right)', \left(h^{(2)}\right)''\right)$ of the 6-dimensional phase trajectory of the wave belonging to the family $\gamma^1_{-1,1}$ are shown. It is seen that the projection shown in Fig. 7b is a curve that is similar to the phase trajectory in 3D space of a long periodic first family wave in the homogeneous film [25]. In the latter case a phase trajectory of a long wave belongs to a neighborhood of the solitary wave trajectory of the first family $\gamma^1_{-1,1}$: the trajectory leaves a neighborhood of the fixed point $(1, 0, 0)$ along the unstable two-dimensional manifold and returns

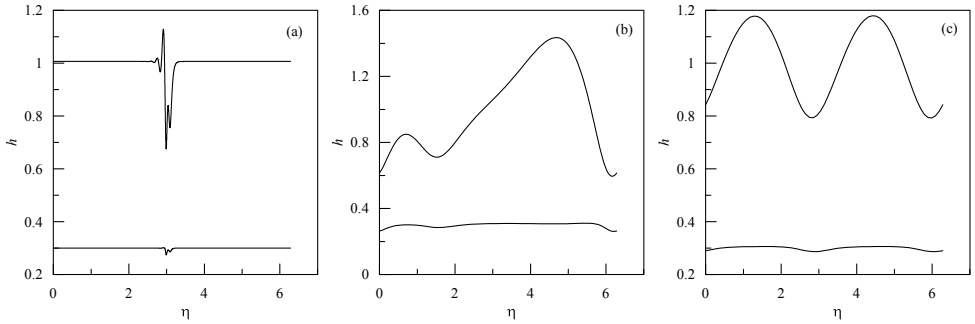

Fig. 8. Examples of waves belonging to the family $\gamma^2_{-2,1}$ at $s = 0.018$ (a), $s = 0.4$ (b) and $s = 0.4616$ (c). Panels (a), (b) and (c) correspond to the points D, E and F, respectively, in Fig. 5.

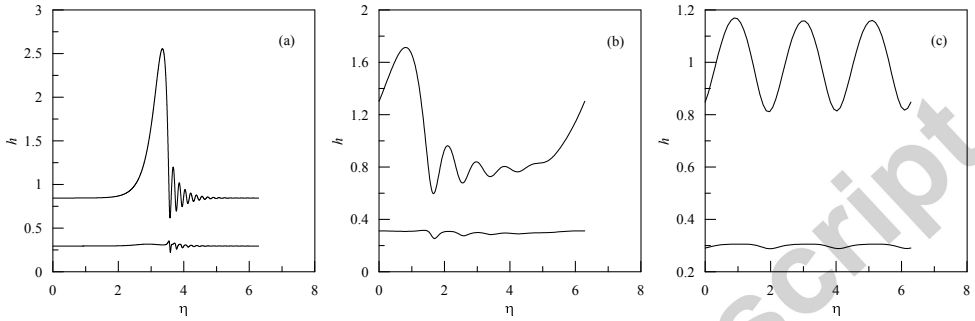

Fig. 9. Examples of waves belonging to the family $\gamma^3_{+1,1}$ at $s = 0.074$ (a), $s = 0.25$ (b) and $s = 0.3125$ (c). Panels (a), (b) and (c) correspond to the points G, H and I, respectively, in Fig. 5.

to the same point along the stable one-dimensional manifold as η varies from $-\infty$ to $+\infty$. It indicates that the extension of the phase space from 3 to 6 weakly affects the projection in $\left(h^{(2)}, \left(h^{(2)}\right)', \left(h^{(2)}\right)''\right)$. The projection shown Fig. 7a demonstrates that there exists other stable and unstable manifolds in the neighborhood of the fixed point $(H, 0, 0, 1, 0, 0)$ in the 6-dimensional space.

Family $\gamma^2_{-2,1}$, see Fig. 5, bifurcates from the first family. At the bifurcation point, the wave is close to the second harmonic, see Fig. 8c. This regular wave corresponds to a limit cycle in the 6-dimensional phase space

$$\left(h^{(1)}, \left(h^{(1)}\right)', \left(h^{(1)}\right)'', h^{(2)}, \left(h^{(2)}\right)', \left(h^{(2)}\right)''\right),$$

and Fig. 8c shows that this family bifurcates from the first family cycle as a period-doubling limit cycle. As the wavenumber s decreases, the shape of the family wave transforms to a solitary-like form, see Fig. 8b and a. Comparing 6a and 8a, we see additional oscillation in the trough of the wave in Fig. 8a.

Period-tripling bifurcation, see Fig. 9c, creates the wave family $\gamma^3_{+1,1}$, see Fig. 5, whose shape at small values of the wavenumber has a large hump (Fig. 9a) in

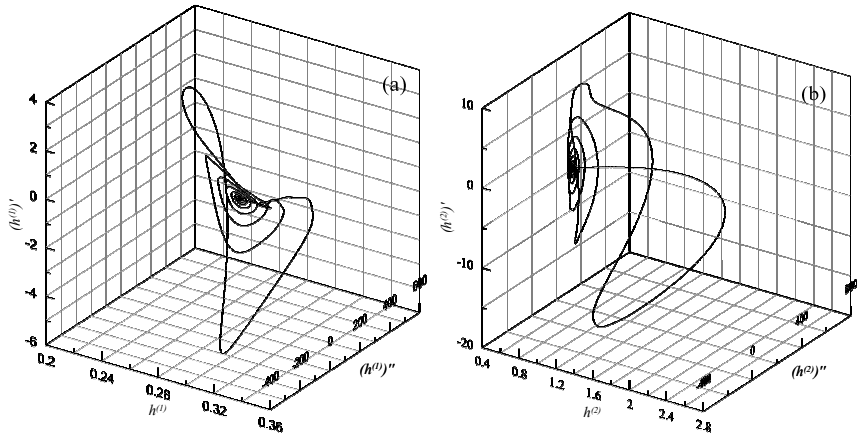

Fig. 10. Projections of 6-dimensional phase trajectory of the family $\gamma^3_{+1,1}$ in 3-dimensional subspace $\left(h^{(1)}, \left(h^{(1)}\right)', \left(h^{(1)}\right)''\right)$ (panel (a)) and $\left(h^{(2)}, \left(h^{(2)}\right)', \left(h^{(2)}\right)''\right)$ (panel (b)) at $s = 0.074$, correspond to the panel (a) in Fig. 9

contrast with the long waves of the families $\gamma^1_{-1,1}$ and $\gamma^2_{-2,1}$. This hump is also observed in shape of intermediate waves of the family (Fig. 9b). We can also analyze the projections in 3-dimensional subspaces $\left(h^{(1)}, \left(h^{(1)}\right)', \left(h^{(1)}\right)''\right)$ and $\left(h^{(2)}, \left(h^{(2)}\right)', \left(h^{(2)}\right)''\right)$ of the trajectory of a long wave belonging to the family $\gamma^3_{+1,1}$, see Fig. 10. This projection is also similar to the corresponding solution of the so-called second family in the homogeneous film, see [25].

In the shown results at $H = 0.3$ the amplitude of the interface waves is respectively small in comparison with the wave amplitudes on the free surface. It is consistent with the fact that these waves bifurcates from the waveless flow similar to the waves in the homogeneous film, see Fig. 1 in [20]. To understand the role of the parameter H, we demonstrate the bifurcation scheme at $H = 0.7$ in Fig. 11. Comparison with the case $H = 0.3$ (Fig. 5) shows that increasing H leads to swapping their bifurcation points by the families $\gamma_{-2,1}$ and $\gamma_{+1,1}$, and this effect is inherent for the wave families in film flows when a similarity parameter varies. Detailed description of the swapping with variation of the film parameter δ can be found in [21].

Examples of waves belonging to different families at $H = 0.7$ are shown in Fig. 12. It is seen that in all cases the interface wave almost imitates the surface wave, and their amplitudes are close. The projections of the phase trajectories in 3D-subspaces confirm that the amplitudes of the pairs $h^{(1)}$ and $h^{(2)}$, $\left(h^{(1)}\right)'$ and $\left(h^{(2)}\right)'$, and $\left(h^{(1)}\right)''$ and $\left(h^{(2)}\right)''$ have the same order.

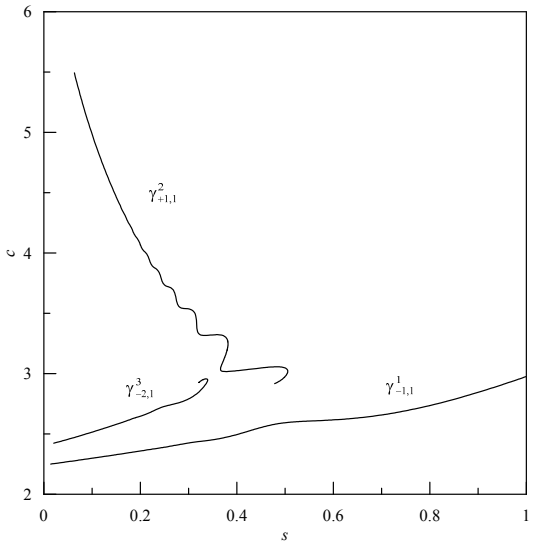

Fig. 11. Bifurcation scheme of the wave families at $\delta = 0.1$ and $H = 0.7$.

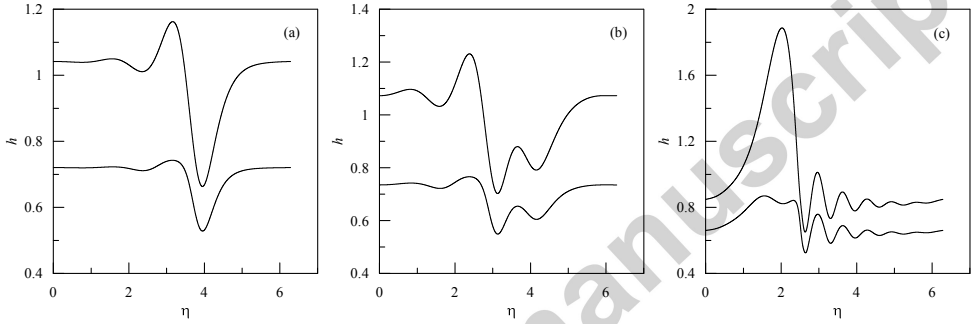

Fig. 12. Examples of waves belonging to the families $\gamma^1_{-1,1}$ (a), $\gamma^3_{-2,1}$ (b) and $\gamma^2_{+1,1}$ (c) at $s = 0.2$, $\delta = 0.1$ and $H = 0.7$.

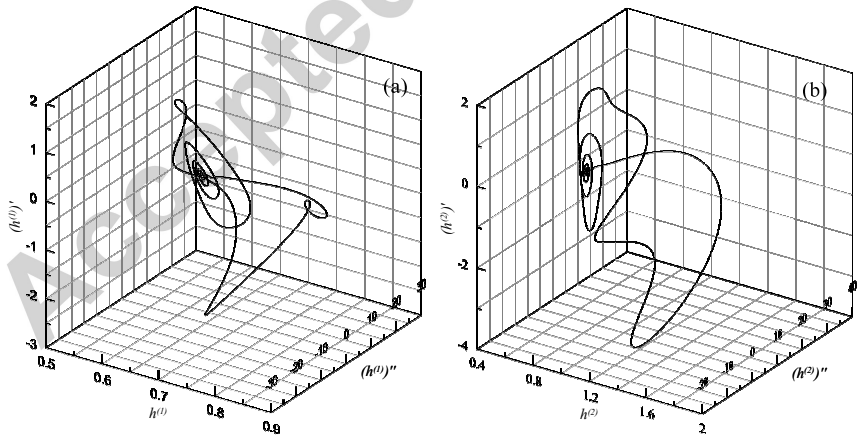

Fig. 13. Projections of 6-dimensional phase trajectory of the family $\gamma^2_{+1,1}$ in 3-dimensional subspace $\left(h^{(1)}, \left(h^{(1)}\right)', \left(h^{(1)}\right)''\right)$ (a) and $\left(h^{(2)}, \left(h^{(2)}\right)', \left(h^{(2)}\right)''\right)$ (b) at $s = 0.2$, correspond to the panel (c) in Fig. 12

4 Conclusions

Evolution equations to model a two-layer film flow have been derived. The equations generalize the Kapitza-Shkadov model [14] for the homogeneous film. The linear analysis has shown that the model is in a good agreement with the full Navier-Stokes system.

For the first time, strongly nonlinear waves in a two-layer falling liquid film have been calculated at real-life values of the similarity parameters. The bifurcation scheme of the wave families and wave shapes of the film surface are typical for film flows. The first wave family $\gamma^1_{-1,1}$ bifurcates from the waveless solution, and other found families bifurcate from the first family as period-doubling and period-tripling. Other bifurcating families at smaller wavenumbers can also be computed.

Non-uniqueness of solutions raises a question how to select solutions which can be used for comparison with experimental data. For homogeneous films, this problem has been investigated using two main approaches. The first approach was to investigate the linear stability of nonlinear steady-traveling waves [16,17]. Another approach was used in [20,19] where transient numerical computations were carried out to find attracting flow regimes, so-called dominating waves. Both strategies can be applied in the considered case of the two-layer film in the future.

In contrast to the case of homogeneous film flows, two-layer films also possess the unstable interface mode whose domain of instability is localized at very small values of the wavenumber, and we can expect that there exist other families of steady-traveling waves. Since Kapitza & Kapitza's experiments [12] for homogeneous films it is known that it is impossible to observe steady-traveling periodic waves whose wave lengths exceed some critical value, and it was theoretically explained in [37]. In the case of the two-layer film, the bifurcating scheme at small wavenumbers is more complicated, and attracting regimes in this domain need a special study.

For many years the Kapitza-Shkadov model [14] has been the main tool to explain experimental data and provides modeling the possible flow regimes in homogeneous film flows despite deriving other models, for example [38,39], and developing computer codes for the full Navier-Stokes problem [40]. We expect that the generalized equations (7) for two-layer film flow will also be widely used to model experimental data in the future.

References

[1] T. W. Kao, Stability of two-layer viscous stratified flow down an inclined plane, Phys. Fluids 8 (1965) 812.

[2] C. S. Yih, Stability of liquid flow down an inclined plane, Phys. Fluids 6 (3) (1963) 321–334.

[3] T. W. Kao, Role of the interface in the stability of stratified flow down an inclined plane, Phys. Fluids 8 (1965) 2190.

[4] T. W. Kao, Role of viscosity stratification in the stability of two-layer flow down an incline, J. Fluid Mech. 33 (1968) 561.

[5] G. M. Sisoev, V. Y. Shkadov, Instability of two-layer film flow along an inclined surface, Fluid Dynamics 27 (2) (1992) 160–165.

[6] K. P. Chen, Wave formation in the gravity-driven low-Reynolds number flow of two liquid films down an inclined plane, Phys. Fluids A 5 (12) (1993) 3038–3048.

[7] J. Hu, S. Millet, V. Botton, H. B. Hadid, D. Henry, Inertialess temporal and spatio-temporal stability analysis of the two-layer film flow with density stratification, Phys. Fluids 18 (2006) 104101.

[8] J. Hu, X. Y. Yin, H. B. Hadid, D. Henry, Linear temporal and spatiotemporal stability analysis of the two-layer falling film flows with density stratification, Phys. Rev. E 77 (2008) 026302.

[9] D. S. Loewenherz, C. J. Lawrence, The effect of viscosity stratification on the instability of a free surface flow at low reynolds number, Phys. Fluids A 1 (1989) 1686.

[10] W. Y. Jiang, B. Helenbrook, S. P. Lin, Inertialess instability of a two-layer liquid film flow, Phys. Fluids 16 (2004) 652–663.

[11] P. Gao, X.-Y. Lu, Mechanism of the long-wave inertialess instability of a two-layer film flow, J. Fluid Mech. 608 (2008) 379–391.

[12] P. L. Kapitza, S. P. Kapitza, Wave flow of thin viscous liquid films. III. Experimental study of wave regime of a flow, Journal of Experimental and Theoretical Physics 19 (2) (1949) 105–120.

[13] P. L. Kapitza, Wave flow of a thin viscous fluid layer. I. Free flow, Journal of Experimental and Theoretical Physics 18 (1) (1948) 3–20.

[14] V. Y. Shkadov, Wave flow regimes of a thin layer of viscous fluid subject to gravity, Fluid Dynamics 2 (1) (1967) 29–34.

[15] A. V. Bunov, E. A. Demekhin, V. Y. Shkadov, On the nonuniqueness of nonlinear wave solutions in a viscous layer, J. Appl. Math. Mech. 48 (4) (1984) 691–696.

[16] Y. Y. Trifonov, O. Y. Tsvelodub, Nonlinear waves on the surface of a falling liquid film. Part 1. Waves of the first family and their stability, J. Fluid Mech. 229 (1991) 531–554.

[17] O. Y. Tsvelodub, Y. Y. Trifonov, Nonlinear waves on the surface of a falling liquid film. Part 2. Bifurcations of the first-family waves and other types of nonlinear waves, J. Fluid Mech. 244 (1992) 149–169.

[18] H.-C. Chang, E. A. Demekhin, D. L. Kopelevich, Nonlinear evolution of waves on a vertically falling film, J. Fluid Mech. 250 (1993) 433–480.

[19] G. M. Sisoev, V. Y. Shkadov, Development of dominating waves from small disturbances in falling viscous-liquid films, Fluid Dynamics 32 (6) (1997) 784–792.

[20] G. M. Sisoev, V. Y. Shkadov, Dominant waves in a viscous liquid flowing in a thin sheet, Doklady-Physics 42 (12) (1997) 683–686.

[21] G. M. Sisoev, V. Y. Shkadov, A two-parameter manifold of wave solutions to an equation for a falling film of a viscous fluid, Doklady-Physics 44 (7) (1999) 454–459.

[22] V. Y. Shkadov, G. M. Sisoev, Waves induced by instability in falling films of finite thickness, Fluid Dynamics Research 35 (5) (2004) 357–389.

[23] G. M. Sisoev, Bifurcation of attractor in falling film problem, International Journal on Non-Linear Mechanics 43 (2008) 246–263.

[24] S. V. Alekseenko, V. E. Nakoryakov, B. T. Pokusaev, Wave Flow of Liquid Films, Begel House, Inc., New York, 1994, 313pp.

[25] H.-C. Chang, E. A. Demekhin, Complex Wave Dynamics on Thin Films, Elsevier, Amsterdam, 2002, 412pp.

[26] C.-S. Yih, Instability due to viscosity stratification, J. Fluid Mech. 27 (2) (1967) 337–352.

[27] A. P. Hooper, W. G. C. Boyd, Shear-flow instability at the interface between two viscosity fluids, J. Fluid Mech. 128 (1983) 507–528.

[28] E. J. Hinch, A note on the mechanism of the instability at the interface between two shearing fluids, J. Fluid Mech. 144 (1984) 463–465.

[29] A. P. Hooper, Long-wave instability at the interface between two viscous fluids: thin layer effects, Phys. Fluids 28 (6) (1985) 1613.

[30] A. P. Hooper, R. Grimshaw, Nonlinear instability at the interface between two viscous fluids, Phys. Fluids 28 (1) (1985) 37–45.

[31] R. M. Roberts, Y. Ye, E. A. Demekhin, H.-C. Chang, Wave dynamics in two-layer couette flow, Chem. Eng. Sci. 55 (2000) 345–362.

[32] G. M. Sisoev, C. J. Bennett, Solitary and transitional waves in gravity-driven two-layer microchannel flow, Fluid Dynamics Research 45 (2013) 015503.

[33] G. M. Sisoev, C. J. Bennett, Solitary and transitional waves in pressure-driven two-layer microchannel flow, Fluid Dynamics Research 46 (2014) 025504.

[34] M. Renardy, Y. Y. Renardy, Derivation of amplitude equations ana analysis of sideband instabilities in two-layer flows, Phys. Fluids A 5 (2005) 2738–2762.

[35] C. T. Gallagher, D. T. Leighton, M. J. McCready, Experimental investigation of a two-layer shearing instability in a cylindrical couette cell, Phys. Fluids 8 (9) (1996) 2385–2392.

[36] Y. Zhao, G. Chen, Q. Yuan, Liquid-liquid two-phase flow patterns in a rectangular microchannels, AIChE J. 52 (12) (2006) 4052–4060.

[37] V. Y. Shkadov, G. M. Sisoev, On the theory of solitary waves in flowing-down layer of viscous fluid, Doklady-Physics 46 (10) (2001) 760–764.

[38] C. Ruyer-Quil, P. Manneville, Improved modeling of flows down inclined planes, Eur. Phys. J. B 15 (2000) 357–369.

[39] C. Ruyer-Quil, P. Manneville, Further accuracy and convergence results on the modelling of flows down inclined planes by weighted-residual approximations, Phys. Fluids 14 (1) (2002) 170–183.

[40] T. R. Salamon, R. C. Armstrong, R. A. Brown, Travelling waves on inclined films: numerical analysis by the finite element method, Phys. Fluids 6 (1994) 2202–2220.